K-band phased-array antenna system demonstration using substrate guided wave true-time delay

Yihong Chen, MEMBER SPIE
Ray T. Chen, FELLOW SPIE
University of Texas at Austin
Microelectronics Research Center
Austin, Texas 78758
E-mail: yhchen@mail.utexas.edu

Abstract. A novel 3-bit optical true-time delay module that can provide 64 time delays ranging from 0 to 443.03 ps is presented. The total insertion loss, including the propagation loss and the 1-to-64 fan-out loss is confirmed to be less than 20 dB. The crosstalk among channels is measured to be less than −40 dB. The bandwidth of the fully packaged module is determined to be as high as 539 GHz. This true-time delay module is employed to control an eight-element K-band phased array antenna system. Far-field patterns covering 18 to 26.5 GHz are measured and compared with the simulated results to verify this module's wide instantaneous bandwidth. *© 2003 Society of Photo-Optical Instrumentation Engineers.* [DOI: 10.1117/1.1578084]

Subject terms: phased-array antenna; true-time delay; substrate-guided wave; holographic optical element.

Paper 020118 received Apr. 1, 2002; revised manuscript received Nov. 6, 2002; accepted for publication Dec. 13, 2002.

1 Introduction

Phased-array antennas (PAAs) have the advantages of low visibility, high directivity, and quick steering. Each antenna element of a PAA must have the correct phase condition to accomplish the desired beam scanning. However, the conventional electrical phase trimmer technique is an intrinsic narrow-band technique that introduces beam squint. Recently, there has been growing interest in optical true-time delay (TTD) modules. Optical TTD techniques are promising for squint-free beam steering of PAAs with features of wide bandwidth, compact size, reduced weights, and low electromagnetic interference. Many kinds of optical TTD techniques have been proposed. These include the acousto-optic technique,[1] the Fourier optics technique,[2,3] the wavelength-multiplexing technique,[4,5] free-space techniques,[6,7] planar waveguide techniques,[8–10] the fiber delay line technique,[11] and the chirped fiber grating technique.[12] However, these modules are for applications with low rf frequencies, limited resolution, and complicated structures for steering control.

In this paper, a new TTD module having time delay steps ranging from 0 to 443.03 ps is designed, fabricated, and packaged. The insertion loss of this module is measured. The time delay error and bandwidth of the packaged device are specified. This module is employed to control an eight-element K-band PAA system. The wide instantaneous bandwidth of the TTD module is confirmed by measurements of far-field patterns covering 18 to 26.5 GHz.

2 Structure of the TTD Module

Figure 1 illustrates the structure of the TTD module. This module is composed of eight subunits. The optical signal, encoded by a microwave signal, is distributed among the eight subunits using a 1-to-8 splitter. Each of the subunits has a wedge of 21.5 deg, as indicated in Fig. 1. The wedges are coated with 50-nm aluminum deposited by e-beam to ensure that more than 98% optical power is confined in the substrate. The wedge angle introduces a bounce angle that is larger than the total internal reflection angle (41.8 deg) at the interface of the substrate (BK-7 glass) and air. Adjacent to each wedge, the height of each subunit is maintained at the same value of t. The height of each subunit varies after one zigzag bounce and is maintained at a fixed value for the rest of the subunit. The heights of the eight subunits after the first zigzag bounce are from h_1 to h_8, with a difference of Δh between adjacent subunits. The difference Δh is preselected to satisfy the required delay combinations. The input signals from single-mode optical fibers are coupled into the module using GRIN lenses. The substrate-guided wave zigzags within the substrate through total internal reflection. A portion of the substrate guided wave is extracted each time the wave encounters the output holographic-grating coupler. The extracted optical waves are focused back into optical fibers using GRIN lenses. To avoid affecting total internal reflection boundary conditions and damaging the holographic-grating coupler, there is a space between the GRIN lens and corresponding holographic-grating coupler. From Fig. 1, we can see that an 8×8 matrix of time delays is obtained. Figure 2 shows the 2-D view of this TTD module to illustrate how to calculate achievable delay intervals. The position of delay signals in the delay matrix is depicted by (i,j), where i is the row number, and j is the column number. Assuming the wedge angle is θ, the introduced time delay between signals at (i,j) and (k,l) is given by

$$\tau = \frac{2n}{c\cos(2\theta)}[(l-1)h_k-(j-1)h_i], \tag{1}$$

 0091-3286/2003/$15.00 © 2003 Society of Photo-Optical Instrumentation Engineers

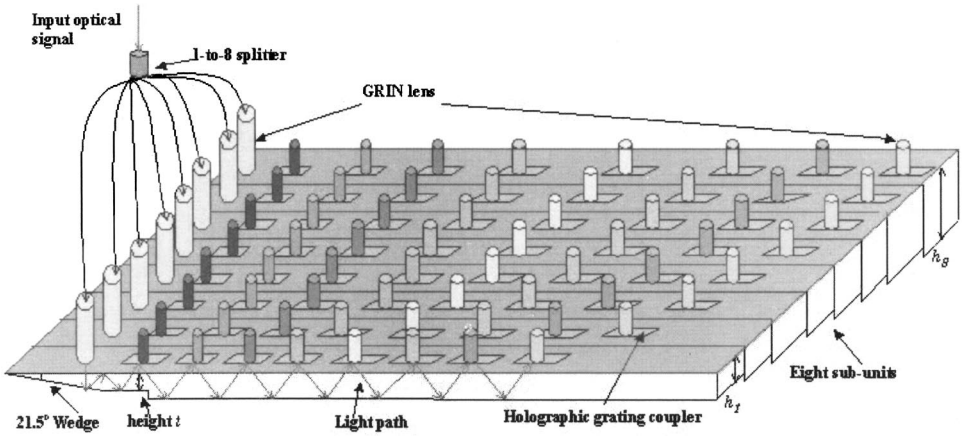

Fig. 1 Diagram of the structure of the 3-bit TTD module based on substrate-guided wave and holographic-grating couplers: GRIN, graded index.

where c is the velocity of light in free space, n is the refractive index of the substrate, h_i is the height of the ith substrate, and h_k is the height of the k'th substrate.

Dupont photopolymer film HRF600*14-20 was used to form the holographic gratings. BK-7 glass was employed as the guided wave substrates. The surface dimension of each subunit is 90×11 mm. The step height t is 2.6 mm. The height difference between the adjacent substrates is 0.147 mm. The heights after the first bounce of the eight substrates are 3.600, 3.747, 3.894, 4.041, 4.188, 4.335, 4.482, and 4.629 mm, respectively. Therefore, the volume of this module is $90\times88\times4.63$ mm. The 8×8 2-D time delay matrix is shown in Table 1. The unit of time delays in Table 1 is 1 ps. Time delays are calculated with reference to the first column of the delay matrix, providing time delays ranging from 0 to 443.03 ps.

The relationship between the time delay interval Δt and the corresponding antenna steering angle can be expressed as[13]

$$\theta=\sin^{-1}[c(\Delta t/d)], \tag{2}$$

where c is the velocity of light in free space, Δt is the time delay interval between adjacent antenna elements, and d is the space interval of adjacent antenna elements. By taking a derivative of the scanning angle with respect to the time delay, we can write the resolution of the scanning angle with respect to the resolution of the time delay interval as

$$\delta\theta=\frac{c\,\delta t}{d\cos\theta}, \tag{3}$$

where c is the velocity of light in free space, $\delta\theta$ is the resolution of the scanning angle, δt is the resolution of the time delay interval, d the space interval of adjacent antenna elements, and θ the steering angle of a PAA.

The K-band PAA used in the experiment has eight elements with a spacing interval of 0.3 in. between adjacent elements. By employing the TTD settings for beam-squint-free phased-array steering, we are able to calculate possible degrees of the steering of the K-band PAA to be 0, 4.5, 9.1, 13.7, 18.5, 23.3, 28.3, and 33.6 deg, as long as the columns of the matrix are used to provide delay steps as shown in Table 1. Even wider scanning range can be achieved with more subunits or higher substrates.

This module is designed to control eight antenna elements with eight possible steering angles. For more antenna elements, more substrates are employed. Furthermore, for more steering angles, more fan-outs are coupled out. For large arrays, optical amplifiers that can provide more than 40 dB gain will be adopted to compensate for the optical insertion loss. Compared to a 1×64 fiber splitter delay lines, the preceding substrate-guided-wave module is able to provide high-resolution time delays (0.01 ps), which is tremendously difficult for common fiber cutting and splicing techniques.

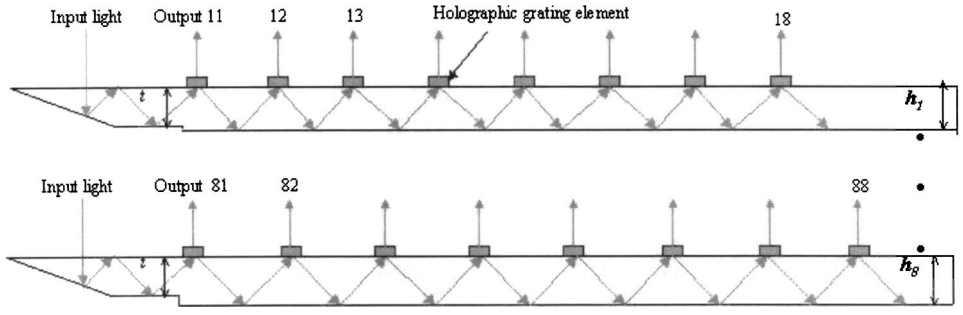

Fig. 2 Two-dimensional view of the TTD module.

Table 1 The delay matrix and corresponding scanning angles of the TTD module.

	Column							
Row	1	2	3	4	5	6	7	8
1	0	49.22	98.44	147.66	196.88	246.10	295.32	344.54
2	0	51.23	102.46	153.69	204.92	256.15	307.38	358.61
3	0	53.24	106.48	159.72	212.96	266.20	319.44	372.68
4	0	55.25	110.50	165.75	221.00	276.25	331.50	386.75
5	0	57.26	114.52	171.78	229.04	286.30	343.56	400.82
6	0	59.27	118.54	177.81	237.08	296.35	355.62	414.89
7	0	61.28	122.56	183.84	245.12	306.40	367.68	428.96
8	0	63.29	126.58	189.87	253.16	316.45	379.74	443.03
Delay steps	0	2.01	4.02	6.03	8.04	10.05	12.06	14.07
Scan angles (deg)	0	4.5	9.1	13.7	18.5	23.3	28.3	33.6

Unit of time delay: 1 ps.

3 Characteristics of the TTD Module

To achieve uniform fan-out beams from each subunit, the diffraction equation of the ith and the $i+1$th holograms have to satisfy the following equation:

$$\eta_{i+1}=\frac{\eta_i}{1-\eta_i}, \tag{4}$$

where η_i is the efficiency of the ith holographic-grating coupler, and η_{i+1} is the efficiency of the $i+1$th holographic-grating coupler.

Notice that the achievable maximum efficiency of the HRF600*14-20 photopolymer at 1550 nm is 40%, the efficiencies of the eight holographic-grating couplers on each subunit are designed as 10.5, 11.7, 13.3, 15.4, 18.2, 22.2, 28.6, and 40% sequentially. The corresponding 64 fan-out spots are shown in Fig. 3 in 2-D format. To further determine the uniformity of the insertion loss, powers of fan-out beams from all eight subunits were accurately measured, and the total insertion loss, including the propagation loss and the 1-to-64 fan-out loss was experimentally confirmed to be less than 20 dB. The crosstalk between channels was measured to be less than -40 dB.

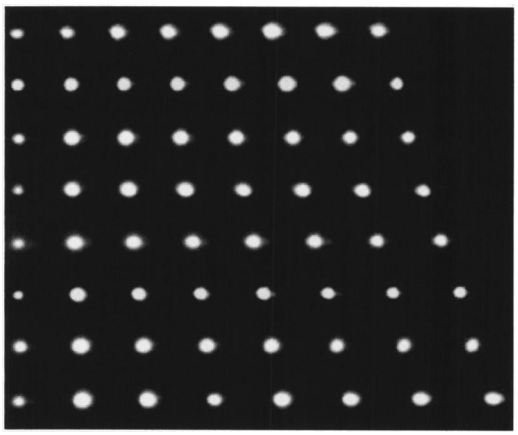

Fig. 3 Sixty-four fan-outs from the TTD module.

The delay intervals were measured using a FPL-01T femtosecond Er-fiber laser from Calmar Optcom Inc., providing optical pulses around 0.2 ps in the vicinity of 1550 nm. Figure 4 illustrates the diagram of the experimental setup for measuring delay intervals. The delay signals are fed into an HP 83480A digital oscilloscope with a resolution of 0.01 ps. Since the HP 83480A digital oscilloscope can detect signals only up to 40 GHz, the detected pulses were broadened to 25 ps. Due to this broadening effect, small delay intervals of several picoseconds can not be shown by the digital oscilloscope. However, since every bounce inside one subunit introduces a same delay, instead of measuring every delay interval in Table 1, we measured the delay interval between the (1,8) fan-out and the (8,8) fan-out. As shown in Fig. 5, the measured delay interval is 98.49 ps, which is the same with the designed value (443.03 ps minus 344.54 ps).

Since the module may be used in field demonstration, the temperature effect on the module must be evaluated. The index of BK-7 glass has a temperature coefficient (dn/dT) of 5×10^{-6}. When the temperature varies from -25 to 75°C (±50°C deviation from room temperature), the index will have a change of ±0.00025. According to Eq. (1), the maximum change of time delay interval happens to the eighth column in Fig. 1, and the change is ±0.0023 ps. This change generates a maximum scanning shift of ±1.2 s, as implied by Eq. (3). This error is so small that it will not degrade the system performance seriously.

To determine the maximum frequency range of the mi-

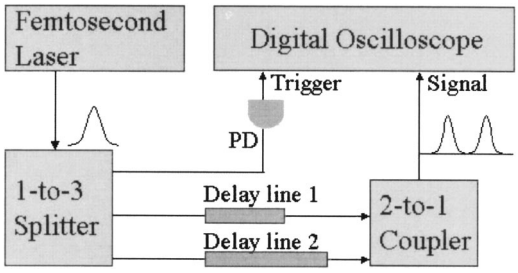

Fig. 4 Diagram of the experimental setup for measuring delay intervals. PD: photodetector.

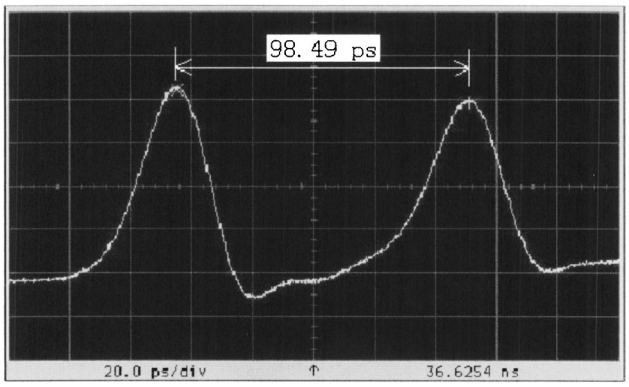

Fig. 5 Measured delay interval between (1,8) fan-out and (8,8) fan-out.

crowave signals that can be carried by the TTD module, the bandwidth of the packaged device is specified. There are three main factors that decide the dispersion capacity of this TTD module. One is the dispersion caused by holographic-grating couplers. The second factor comes from the dispersion of GRIN lens and optical fibers. The third one is material dispersion caused by different phase velocities of different wavelengths. To evaluate the real bandwidth of this TTD module, a femtosecond laser and the Fourier spectrum analysis method were employed.[14] The same femtosecond laser was used as in the delay measurement. A FR-103MN autocorrelator from Femtochrome Research Inc. was adopted to measure pulse widths before and after passing the fully packaged TTD module. The output signal from the autocorrelator is processed and displayed by a computer. Figure 6(a) depicts the autocorrelation traces of the reference and dispersed pulses, respectively. Fourier transform of the two pulses generates bandwidth information of this TTD module, as shown in Fig. 6(b). As can be seen in Fig. 6(b), the 3-dB bandwidth of the device is 539 GHz.

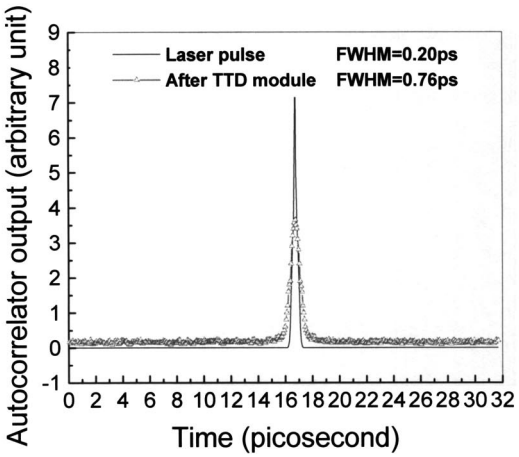

(a)

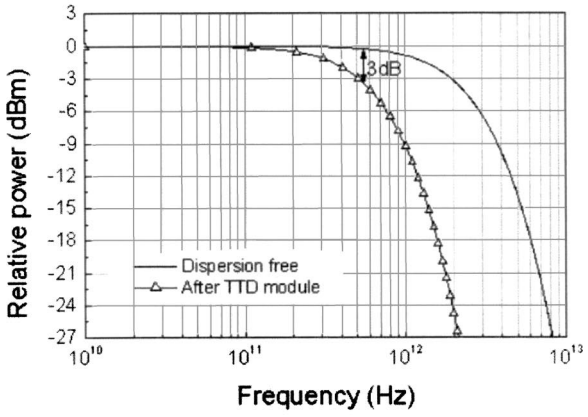

(b)

Fig. 6 (a) Autocorrelation traces of the pulses before and after passing the TTD module and (b) fast Fourier transform (FFT) power spectrum for the reference and dispersed pulses.

4 System Integration

Packaging is always a challenging task for photonic devices. In this module, there are two crucial issues to minimize the packaging insertion loss; they are the performance of the coupling lenses and the alignment among the TTD substrates and the coupling lenses. Since the minimum distance between adjacent output beam centers is only 6.7 mm, the package requires small outside-diameter (OD) fiber collimating and focusing lenses. In our package, the divergence angle (DA) and beam diameter (BD) needed to be as small as possible to minimize the packaging size and to minimize the beam spot size after eight bounces within the substrate. It is obvious that small core-size fiber and a lens with a long focal length will collimate well. However, long focal length requires a large-diameter lens and produces a large beam spot. Having these constraints in mind, the input fiber collimator lenses were designed[14] with a BD of 0.8 mm and a DA of 0.1 deg. Several special mechanisms were designed to align the optical lenses with the substrates. Each subunit is packaged separately. The input fiber collimator is mounted on a tilt flange, which has a resolution of 0.01 deg and can be easily tuned with screwdrivers, with the accuracy determined by the thread spacing. The eight output fiber focusers are mounted on a large piece of tilt flange, with a resolution of 0.005 deg. The substrate is held by a 2-D moving stage to ensure that the beam spots from the substrate are centered at the core of the lenses. The packaged TTD module is shown in Fig. 7 with one column fan-out coupled out.

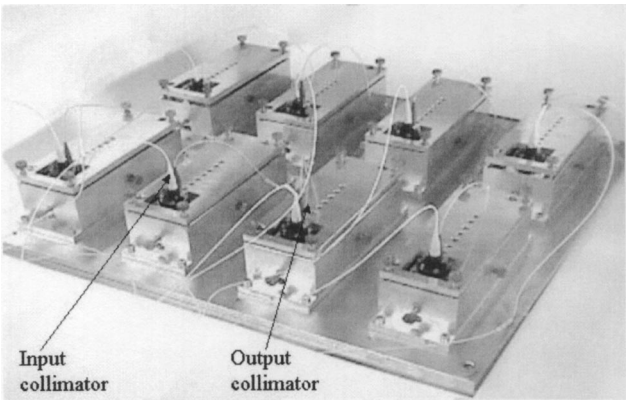

Fig. 7 Photograph of the packaged 3-bit TTD module.

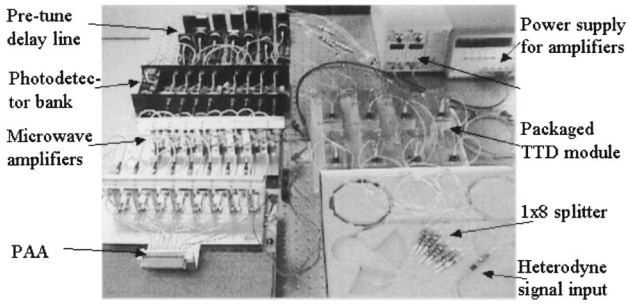

(a)

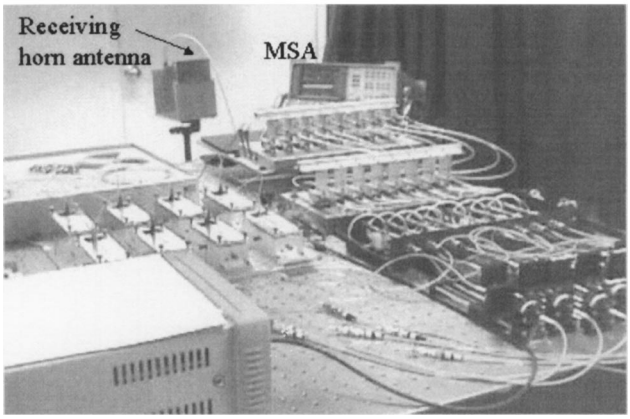

(b)

Fig. 8 Photograph of the integrated K-band PAA system: (a) Photograph of the transmission part of the PAA system and (b) Photograph of the PAA system with a standard horn receiver. MSA: microwave spectrum analyzer.

The integrated K-band PAA system is demonstrated in Fig. 8. Figure 8(a) shows the transmission part of the system. Figure 8(b) shows both the transmitter and the horn antenna receiver. A microwave signal is generated by the heterodyne technique using two external-cavity tunable semiconductor lasers. The optical carriers are evenly distributed among the eight subunits of the TTD module by a 1-to-8 splitter. Desired time delays are added by this TTD module. Since to cut and splice an optical fiber with accuracy of 3 μm (corresponding to a 0.01-ps propagation time) is extremely difficult, a preadjustment delay bank with eight preadjustment delay lines are inserted at this point to compensate for the different lengths of fiber pigtailed devices. Afterward, the microwave signals are detected by InGaAs high-speed photodetectors. The eight microwave signals with correct phase relationship are fed into eight antenna elements individually after amplification. The on/off states of photodetectors are controlled by a printed circuit board, which also serves as a microwave power uniformity controller. The photodetector outputs of the same row are connected to an antenna element. For single-angle scanning of this K-band PAA, only photodetectors from the specified column are selected. In a multibeam application, photodetectors from multiple columns will be chosen.

5 Far-Field Pattern Measurements

Far-field patterns of the K-band PAA were measured to verify the instantaneous microwave broad bandwidth. Various delay combinations were tested. Far-field patterns were measured at three frequencies, the center frequency (22 GHz) and two edge frequencies (18 and 26.5 GHz). Figure 9 compares the far-field patterns at the three frequencies, with solid curves and curves with triangles denoting simulated results and measured results, respectively. Note that in Fig. 9, the fifth column of the TTD module shown in Fig. 1 is employed to provide delay control signals for 18.5-deg scanning of the PAA. The locations of the mainlobes covering all K-band resulted from simulation and experiment agree very well. Furthermore, the PAA scanning angle is independent of microwave frequencies over the entire K-band, a primary feature of the TTD approach.

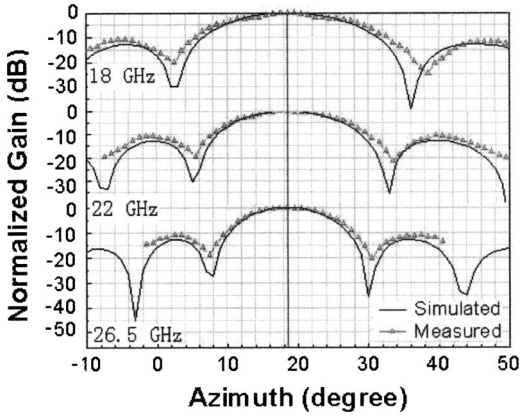

Fig. 9 Comparison of far-field patterns at three different frequencies: 18, 22, and 26.5 GHz.

6 Conclusion

In conclusion, a novel 3-bit optical TTD module that can provide 0 to 443.03 ps time delay was fabricated, packaged, and integrated into a K-band PAA system. This module has an insertion loss of less than 20 dB, a crosstalk of less than −40 dB, and a bandwidth of 539 GHz. This module is compact, easy to fabricate, and was experimentally confirmed to provide a wide instantaneous microwave bandwidth. By modifying the height difference and refractive angle, this module can be employed to control PAAs at wider frequency bands.

Acknowledgment

The authors would like to thank Dr. Juergen Pohlmann of MDA and Dr. Charles Lee of AFOSR for their support and encouragement.

References

1. L. H. Gesell, R. E. Feinleib, J. L. Lafuse, and T. M. Turpin, "Acousto-optic control of time delays for array beam steering," in *Optoelctronic Signal Processing for Phased-Array Antennas IV*, *Proc. SPIE* **2155**, 194–204 (1994).
2. Y. Konishi, W. Chujo, and M. Fujise, "Carrier-to-noise ratio and sidelobe level in a two-laser mode optically controlled array antenna using Fourier optics," *IEEE Trans. Antennas Propag.* **40**, 1459–1465 (1992).
3. G. A. Koepf, "Optical processor for phased-array antenna beam formation," *Proc. SPIE* **477**, 75–81 (1984).
4. D. T. K. Tong and M. C. Wu, "A novel multiwavelength optically controlled phased array antenna with a programmable dispersion matrix," *IEEE Photonics Technol. Lett.* **8**, 812–814 (1996).
5. R. Esman, M. Frankel, J. Dexter, L. Goldberg, M. Parent, D. Stiwell, and D. Cooper, "Fiber-optic prism true time-delay antenna feed," *IEEE Photonics Technol. Lett.* **5**, 1347–1349 (1993).

6. H. R. Fetterman, Y. Chang, D. C. Scott, S. R. Forrest, F. M. Espiau, M. Wu, D. V. Plant, J. R. Kelly, A. Matteer, and W. H. Steier, ''Optically controlled phased array radar receiver using SLM switched real time delays,'' *IEEE Microw. Guid. Wave Lett.* **5**, 414–416 (1995).
7. D. Dolfi, P. Joffre, J. Antoine, J. Huignard, D. Phillippet, and P. Granger, ''Experimental demonstration of a phased-array antenna optically controlled with phase and time delays,'' *Appl. Opt.* **35**, 5293–5300 (1996).
8. E. Ackerman, S. Wanuga, D. Kasemset, W. Minford, N. Thorsten, and J. Watson, ''Integrated 6-bit photonic true-time-delay unit for lightweight 3–6 GHz radar beamformer,'' *IEEE Trans. Microwave Theory Tech.* **6**, 681–684 (1992).
9. K. Horikawa, I. Ogawa, H. Ogawa, and T. Kitoh, ''Photonic switched true time delay beam forming network integrated on silica waveguide circuits,'' *IEEE MTT-S Int. Microwave Symp. Dig.* **TU1C-6**, 65–68 (1995).
10. W. Wang, Y. Shi, W. Lin, and J. H. Bechtel, ''Waveguide binary photonic true-time delay lines using polymer integrated switches and waveguide delays,'' *Proc. SPIE* **2844**, 200–211 (1996).
11. W. Ng, A. A. Walston, G. L. Taughlian, J. J. Lee, I. L. Newberg, and N. Bernstein, ''The first demonstration of an optically steered microwave phased array antenna using true-time-delay,'' *J. Lightwave Technol.* **9**, 1124–1131 (1991).
12. J. L. Corral and J. Marti, ''Optical up-conversion on continuously variable true-time-delay lines based on chirped gratings for millimeter-wave optical beamforming networks,'' *IEEE Trans. Microwave Theory Tech.* **47**, 1315–1320 (1999).
13. A. A. Oliner and G. H. Knittel, *Phased Array Antennas*, Artech House, Norwood, MA (1972).
14. Y. Chen, ''Waveguide-hologram-based true-time delay modules for K-band phased-array antenna system demonstration,'' PhD Dissertation, University of Texas at Austin (2002).

Yihong Chen received her BE and ME degrees in microwave telecommunications from the XiDian University, and her PhD in optical communications from the Beijing University of Posts and Telecommunications in 1999. To continue research interest in optical communications, she joined the optoelectronic interconnects group at the University of Texas at Austin and received a PhD degree in 2002. She is currently with Omega Optics, Inc. Her research work in the past 5 years has focused on phased-array antenna theory, optical true-time delay feeding networks for phased-array antennas, and system integration of phased-array antennas.

Ray. T. Chen is the Temple Foundation Endowed Professor in the Department of Electrical and Computer Engineering, the University of Texas at Austin (UT Austin). His research group has been awarded more than 60 research grants and contracts from such sponsors as the Department of Defence (DOD), the National Science Foundation (NSF), the Department of Energy (DOE), the National Aeronautios and Space Administration (NASA), the State of Texas, and private industry. The research topics include guided-wave and free-space optical interconnects, polymer-based integrated optics, a polymer waveguide amplifier, graded-index polymer waveguide lenses, an active optical backplane, a traveling-wave electro-optic polymer waveguide modulator, optical control of phased-array antenna, a GaAs all-optical crossbar switch, holographic lithography, and holographic optical elements. The optical interconnects research group at UT Austin has reported its research in more than 250 published papers. He has chaired or been a program committee member for more than 40 domestic and international conferences, organized by SPIE, OSA, IEE, and PSC. He has served as a consultant for various federal agencies and private companies and delivered numerous invited talks to professional societies. Dr. Chen is a fellow of the SPIE and the Optical Society of America, a senior member of IEEE/LEOS, and a member of PSC. There are currently 20 PhD degree students and seven postdoctors working in Chen's group.